

# Measuring and Modelling Crowd Flows - Fusing Stationary and Tracking Data

Martin Treiber

**Abstract** The two main data categories of vehicular traffic flow, stationary detector data and floating-car data, are also available for many Marathons and other mass-sports events: Loop detectors and other stationary data sources find their counterpart in the RFID tags of the athletes recording the split times at several stations during the race. Additionally, more and more athletes use smart-phone apps generating track data points that are the equivalent of floating-car data. We present a methodology to detect congestions and estimate the location of jam-fronts, the delay times, and the spatio-temporal speed and density distribution of the athlete’s crowd flow by fusing these two data sources based on a first-order macroscopic model with triangular fundamental diagram. The method can be used in real-time or for analyzing past events. Using synthetic “ground truth” data generated by simulations with the Intelligent-Driver Model, we show that, in a real-time application, the proposed algorithm is robust and effective with minimal data requirements. Generally, two stationary data sources and about ten “floating-athlete” trajectories per hour are sufficient.

## 1 Introduction

While vehicular traffic data analysis and flow modeling is a mature research field [1], only few scientific investigations exist for the dynamics and data analysis of unidirectional crowd flow, particularly in mass-sports events. Popular mass-sports events include classical Marathons (e.g., the *New York Marathon*), cross-country events (e.g., the *Vasaloppet* [2]), and other events such as the increasingly popular inline-skating nights (e.g., the *Dresdner Nachtskaten*).

Microscopically, the crowd dynamics can be described either by two-dimensional active-particle systems [3], or by multi-lane one-dimensional traffic flow models for

---

Martin Treiber

Technische Universität Dresden, Würzburger Str. 35, D-01062, Dresden e-mail: treiber@vwi.tu-dresden.de

the case of ski Marathons in the classic style [2]. Unlike the situation in general pedestrian traffic, the flow is (i) unidirectional and (ii) there is no route choice: All athletes remain on the race track from start to finish. This means, the dynamics is equivalent to that of mixed unidirectional vehicular traffic flow on a link [4, 5].

This allows to simplify the mathematical description to a macroscopic, one-dimensional model. The free regime is described in [2]. In the congested regime, most of the individuality is lost. Moreover, genuine “crowd-flow” instabilities (stop-and-go waves) are rare allowing to describe the macroscopic dynamics by Lighthill-Whitham-Richards (LWR) models [6].



Fig. 1: Data basis for Marathon events: Stationary counting data at the stations obtained by RFID chips (left), and “floating athlete data” obtained by smart-phone apps (right).

These models can be calibrated by data that are essentially equivalent to that of vehicular traffic. Loop detectors and other stationary data sources find their counterpart in the RFID tags of the athletes recording the split times at several stations during the race (cf. Fig. 1 left). For our purposes, they are simply counting detectors. Additionally, more and more athletes use smart-phone apps generating, in real time, track data points that are the equivalent of floating-car data (cf. Fig. 1 right). These two data sources complement each other: split-time data are available for all the athletes but only at a few positions. In contrast, “floating-athlete data” cover the whole track but the percentage of athletes with activated smart-phone apps is low and unknown.

In this contribution, we present a methodology to detect congestions, track their upstream fronts in real-time, and reconstruct the spatio-temporal local speed of the crowd flow by fusing these two data sources. The algorithm is based on a LWR

model with tridiagonal fundamental diagram. We calibrate and validate the method based on simulated “ground truth” data generated with the Intelligent-Driver Model (IDM) [7].

In the next section, we develop the estimation methodology, in Sect. 3 we present the simulation results before we conclude this paper with a discussion (Sect. 4).

## 2 Methods

### 2.1 The reconstruction algorithm

The basic algorithm uses only the flow information of two stationary detectors that are located at the upstream and downstream boundary of the section to be analyzed. It is based on the LWR with the triangular fundamental diagram  $Q_e(\rho)$  which can be expressed in terms of the parameters free-flow speed  $V_0$ , maximum flow (capacity)  $Q_{\max}$ , and wave speed  $c$ ,

$$Q_e(\rho) = \begin{cases} V_0 \rho & \text{if } \rho \leq \frac{Q_{\max}}{V_0} \text{ (free flow),} \\ Q_{\max} \left[ 1 - \frac{c}{V_0} \right] + c\rho & \text{if } \rho > \frac{Q_{\max}}{V_0} \text{ (congested flow).} \end{cases} \quad (1)$$

The algorithm for detecting congestions and tracking their upstream fronts is specified completely in Chapter 8.5.8 of [1], cf. also Fig. 2. It uses the facts that (i) in free traffic, flow information is propagated downstream at velocity  $V_0$ , (ii) in congested traffic, the propagation is upstream at velocity  $c$ , (iii) the propagation of the position  $x_{12}(t)$  of the transition free  $\rightarrow$  congested is given by the shock-wave formula

$$\frac{dx_{12}}{dt} = \frac{Q_1 - Q_2}{\rho_1 - \rho_2} \quad (2)$$

where  $Q_1$ ,  $\rho_1$ ,  $Q_2$ , and  $\rho_2$  are expressed in terms of the flows of the upstream and downstream detectors, respectively, taken at delayed times corresponding to the propagation velocities  $V_0$  and  $c$ , respectively.

The *floating-athlete data* (visualized as piecewise linear trajectories in Fig. 2) is used to calibrate the three parameters  $\beta = (V_0, Q_{\max}, c)^T$  of the basic algorithm in real time. Whenever a transition free-congested is recognized by a new trajectory at position  $x_{12}^{\text{traj}}(t_i)$  and time  $t_i$  (black bullets in this figure), the parameters are updated by minimizing the objective function

$$S(\beta) = \sum_i \left( x_{12}^{\text{pred}}(t_i) - x_{12}^{\text{traj}}(t_i) \right)^2. \quad (3)$$

The summation over the squared differences between the predicted and observed jam front locations starts with the first trajectory detecting a jam (e.g. if the speed drops consistently below a speed threshold). To focus on recent data, an exponential

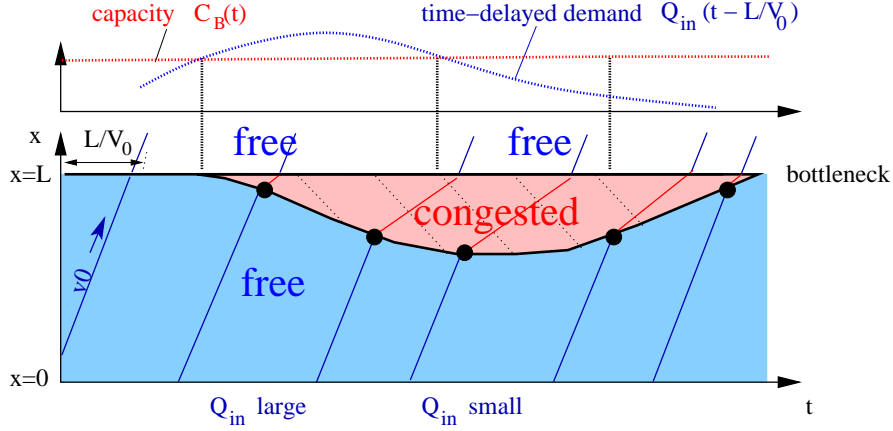


Fig. 2: Schematic visualization of the basic reconstruction algorithm of Sect. 2.1: The flow information  $Q_{in}$  of the upstream detector at  $x = 0$  (demand) propagates downstream through free traffic at velocity  $V_0$  (the density of the lines is proportional to  $Q_{in}$ ) while the information about the bottleneck capacity  $C_B$  (supply) propagates upstream through the congested traffic zone at velocity  $c$  (dotted lines). At the transition, the shock-wave formula applies. Shown are also some *floating-athlete* trajectories.

weighting proportional to  $\exp[(t_i - t)/\tau]$  (where the time scale  $\tau$  should contain a few trajectories) is possible as well.

We emphasize that, even if speed data  $V_i$  are available at detector  $i$ , the algorithm is more robust when the densities in the denominator of the shock-wave formula (2) are calculated using exclusively the detector flows (i.e., the count data) and inverting the fundamental diagram rather than directly estimating the densities by using  $\rho_i = Q_i/V_i$ .

Finally, we notice that this formulation assumes that there is only one transition free-congested between the two stationary detectors. It is most efficient if the downstream detector is located just upstream of a known bottleneck, and the upstream detector is just upstream of the congested region at its maximum extension.

## 2.2 Simulating the ground truth

Since no true ground truth (a complete coverage of the spatio-temporal local speed and flow) is available, the algorithm is tested by simulating the ground truth with a *completely different* model, namely the microscopic intelligent-driver model (IDM) [7] to which some acceleration noise is added to simulate heterogeneity. Particularly, the IDM fundamental diagram is *not* triangular (Fig. 3 right). Because of

their intuitive meaning, it is straightforward to adapt the IDM parameters to directed crowd flows. Specifically, we assumed the parameters of Table 1 representing moderately fast Marathon runners.

Table 1: IDM parameters for moderately fast Marathon runners

parameter	value
width in running direction $l$	0.4 m
maximum speed $v_0$	4.0 m/s
desired time gap $T$	1.0 s
minimum gap $s_0$	0.5 m
gap $s_1$	0.5 m
desired acceleration $a$	$0.5 \text{ m/s}^2$
comfortable deceleration $b$	$1.0 \text{ m/s}^2$

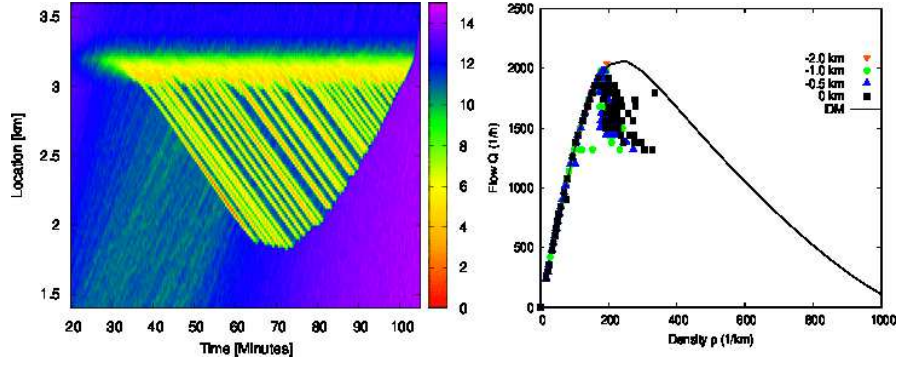


Fig. 3: "Virtual" ground truth as obtained by an IDM simulation. Left: local density; right: flow-density data as obtained from stations at the indicated locations and IDM fundamental diagram.

Figure 3 shows the ground truth as obtained with these parameters in an open system of variable inflow and a bottleneck at  $x = 3.2 \text{ km}$  causing the onset of congestion at about  $t = 25 \text{ min}$ . Notice that the IDM is capable to produce stop-and-go waves also for the crowd-flow parameterization. When increasing the acceleration parameter to  $a = 1 \text{ m/s}^2$ , all flow instabilities vanish.

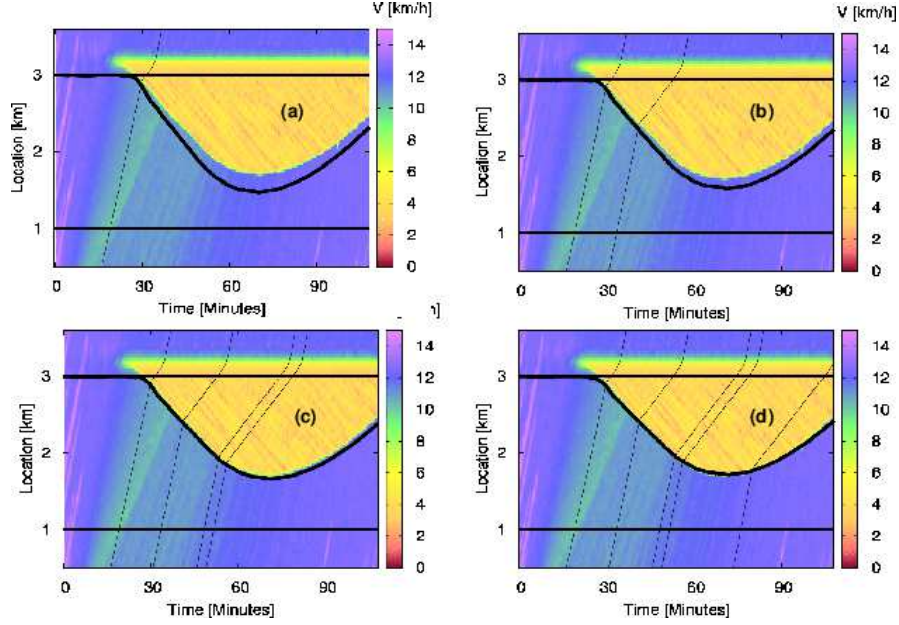


Fig. 4: Real-time calibration and jam front detection of a congestion caused by a bottleneck at  $x = 3$  km. The available information consists of two stationary detectors (horizontal lines) and “floating-athlete” trajectories (dotted curves). For visualization purposes, the (simulated) local ground truth speed is shown color-coded in the background. The jam-front detection algorithm started with the parameters  $v_0 = 10$  km/h,  $c = -5$  km/h, and  $Q_{\max} = 2300$  s $^{-1}$ . (a)-(d) shows the on-line calibration when new floating-athlete trajectories become available. The corrected parameters where (a)  $v_0 = 9$  km/h,  $c = -4.5$  km/h,  $Q_{\max} = 2300$  s $^{-1}$ , (b)  $v_0 = 9$  km/h,  $c = -4.0$  km/h,  $Q_{\max} = 2300$  s $^{-1}$ , (c)  $v_0 = 9$  km/h,  $c = -4.0$  km/h,  $Q_{\max} = 2350$  s $^{-1}$ , and (d)  $v_0 = 9$  km/h,  $c = -4.2$  km/h,  $Q_{\max} = 2440$  s $^{-1}$ . The black curve to the right of the last trajectory shows the jam front that the algorithm would predict just based on the detector data.

### 3 Results

We test the algorithm based on the simulated ground truth generated by the IDM as described in the previous section but with an increased acceleration parameter  $a = 0.8$  m/s $^2$  resulting in stable congested flow. The color-coded background of Fig. 4 depicts the spatio-temporal local speed which is the same in all sub-figures (a)-(d). We assumed two stationary detectors at  $x = 1$  km (upstream of the congestion at any time) and  $x = 3$  km (just upstream of the bottleneck at  $x = 3.2$  km) and started the algorithm at  $t = 0$  (free traffic everywhere). Sub-figure (a) depicts the predicted position of the jam front in the past and future relative to the calibra-



tion using only the first trajectory at  $t = 30$  min. The passage time of the jam front at the downstream detector ( $t \approx 25$  min) is reconstructed correctly while the congestion zone predicted at later times is a little too extended. Subsequent real-time calibrations after transition signals from three further trajectories (subplots (b)-(d)) gradually increase the algorithm's quality.

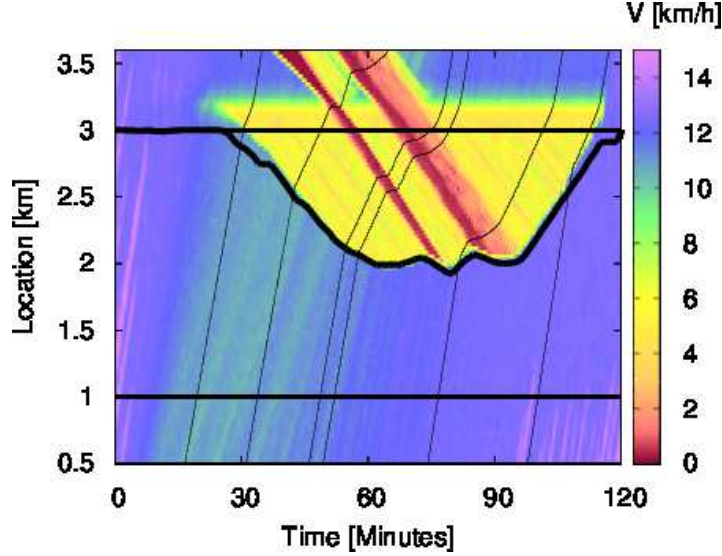


Fig. 5: Validation by predicting the jam front (with unchanged parameters) in a different scenario where an additional jam propagates through the original jam. The floating-athlete data were not used in this test.

Finally, Fig. 5 shows a validation result by applying the algorithm as calibrated in Fig. 4(d) to a new situation where the congestion caused by the bottleneck at  $x = 3.2$  km is superimposed by a more severe congestion (near standstill) caused by a further temporary bottleneck at  $x = 4.0$  km. Even when using *only the two detectors* (the trajectories are only drawn for visual purposes), the maximum error in predicting the location of the jam front is about 200 m and significantly less most of the time.

## 4 Discussion

In this work, I have proposed a traffic state recognition algorithm which is extremely fast (fractions of seconds of computation time for each real-time calibration, much less for a prediction with fixed parameters) and only needs sparse information: two

stationary counting detectors (stations where split times are taken) upstream and downstream of the section to be analyzed, and a few “floating-athlete” trajectories during the period of congestion are sufficient. Since relevant events have of the order of 10 000 participants, this corresponds to a minimum penetration rate of fractions of a percent which is satisfied in most races (cf. Fig. 1 right). By applying the algorithm independently to each section between the two respective neighboring stations, the whole course can be covered. Application of the calibrated algorithm to a new situation results in comparatively low errors demonstrating its robustness.

It is worth noticing that the algorithm ignores all lateral dynamics, i.e., it is based on only the longitudinal dimension. Among others, this allows using car-following models for generating the ground truth although they represent single-file motion rather than true crowd dynamics. The rationale for that is the inherent competitiveness of the athletes always seeking the best lateral position (there is no “go right directive” in racing events) and thereby leveling off lateral differences of the longitudinal speed (i.e., shear rates).

There is evidence that the discrepancy between the free-flow regime of the triangular LWR and the actual free-flow dynamics of the crowd (or the IDM) contributes significantly to the residual errors. This can be improved if the LWR free-flow dynamics is replaced by the dispersion-transport model presented at TGF’13 [8].

In future investigations, the proposed algorithm will be tested using more realistic two-dimensional microscopic crowd flow models to generate the ground truth. It is also planned to test it against the incomplete ground truth obtained from data of real mass-sports events. Finally, we will apply this algorithm to vehicular traffic flow.

## References

1. M. Treiber, A. Kesting, *Traffic Flow Dynamics: Data, Models and Simulation*, Springer, Berlin, 2013.
2. M. Treiber, R. Germ, A. Kesting, From drivers to athletes – modeling and simulating cross-country skiing marathons, in: *Traffic and Granular Flow ’13*, Springer, Berlin, 2015, pp. 243–249.
3. D. Helbing, Traffic and related self-driven many-particle systems, *Reviews of Modern Physics* (2001) 1067–1141.
4. V. Arasan, R. Koshy, Methodology for modeling highly heterogeneous traffic flow, *Journal of Transportation Engineering* 131 (7) (2005) 544–551.
5. V. Kanagaraj, G. Asaithambi, C. Kumar, K. K. Srinivasan, R. Sivanandan, Evaluation of different vehicle following models under mixed traffic conditions, *Procedia-Social and Behavioral Sciences* 104 (2013) 390–401.
6. M. Lighthill, G. Whitham, On kinematic waves: II. A theory of traffic on long crowded roads, *Proc. Roy. Soc. of London A* 229 (1955) 317–345.
7. M. Treiber, A. Hennecke, D. Helbing, Congested traffic states in empirical observations and microscopic simulations, *Physical Review E* 62 (2000) 1805–1824.
8. M. Treiber, Crowd flow modeling of athletes in mass sports events – a macroscopic approach, in: *Traffic and Granular Flow ’13*, Springer, Berlin, 2015, pp. 21–29.